ISSN 1063-7842, Technical Physics, 2017, Vol. 62, No. 6, pp. 882–889. © Pleiades Publishing, Ltd., 2017.
Original Russian Text © V.I. Petinov, 2017, published in Zhurnal Tekhnicheskoi Fiziki, 2017, Vol. 87, No. 6, pp. 867–874.

SOLID STATE

Magnetism of Gadolinium Nanoparticles near T_c

V. I. Petinov

Institute of Problems of Chemical Physics, Russian Academy of Sciences, Chernogolovka, Moscow oblast, 142432 Russia

Received April 28, 2016; in final form, July 13, 2016

Abstract—Influence of temperature and magnetic field H on magnetism of spherical Gd nanoparticles of different sizes (89, 63, 47, 28, and 18 nm) was studied in the temperature range 250 K < T < 325 K. The particles were obtained by metal vapor condensation in the flow of helium. The particles with d = 18 nm did not show a magnetic transition; their structure is a combination of two cubic phases (FCC1 and FCC2). Large particles remained in the HCP phase and had an admixture of the FCC1 phase, the amount of which decreased as the particle sizes increased; magnetic transition took place at T_c = 293 K. The admixture of O_2 did not alter the structure but decreased the magnetization σ and magnetic permeability μ. An orientation transition in polycrystalline gadolinium initiated by the magnetic field H was proved in an experiment. The orientation transition in Gd particles smaller than 63 nm, the magnetic structure of which is close to the single-domain structure, occurred near T_c without the influence of H.

DOI: 10.1134/S1063784217060214

INTRODUCTION

In the last few years magnetic nanoparticles have been widely used in technical [1, 2] and medical [3] applications. Therefore the need for a more detailed study of their properties has arisen [4–12]. Special interest is paid to nanoparticles of gadolinium, which is used in medicine (including MRIs) as a contrast agent [3, 13, 14].

The change in the magnetic state of Gd occurs near the room temperature and, hence, its nanoparticles are a convenient object for studying magnetic transitions in nanocrystals restricted by the size factor. In addition, gadolinium belongs to the group of uniaxial magnetics, which spontaneously change the sign of the first magnetic anisotropy constant at decreasing temperature [15]. This phenomenon is assumed to be an orientation transition, which results in a change of the magnetization direction and, consequently, the symmetry of the magnetic structure [16]. The question arises of whether this transition is possible in gadolinium nanoparticles and how it manifests. Another important question remains open of whether there a single-domain state exists in rare-earth magnetics, including Gd nanoparticles.

The value of T_c of Gd is only 15–20°C lower than the temperature of warm-blooded animals, which can create new vistas in using Gd nanoparticles in medicine and veterinary practice. In particular, they may be used for the targeted localization of drugs in certain places of the organism and the controlled removal of drug compounds using biologically acceptable local gradients of temperature and magnetic field.

In light of the above, a detailed investigation of the magnetic state of Gd nanoparticles near the phase transition temperature and the determination of the dependence of this state on the nanoparticle sizes, temperature, and external magnetic field have to be carried out.

EXPERIMENTAL

In the investigations described below, we used spherical nanoparticles of Gd with the volume average diameters of 89, 63, 47, 28, and 18 nm. In what follows the terms *nanoparticle size* and *nanoparticle diameter* and the value denoted as d always correspond to the volume average diameter of the nanoparticles in a sample, which is defined from the particle size distribution as

$$d = \langle d \rangle_v = (\Sigma n_i d_i^3 / \Sigma n_i)^{1/3}, \quad (1)$$

where n_i is the number of particles with the size of d_i, Σn_i is the total number of nanoparticles being analyzed on electron microscopy images (~500).

Nanoparticles of Gd were obtained by metal vapor condensation in inert gas flow (Gen–Miller method) [17]. High-purity helium was used as the inert carrier gas; the controlled amount of oxygen was added to helium in some cases. More detailed information on the technology of obtaining Gd nanoparticles studied in the present work, their structure, the method of controlling their size, and the influence of the oxygen admixture on their properties and magnetism were published in [18].

The samples were prepared as a suspension of the Gd nanoparticles in paraffin. The relative volume η_v and weight α_m fractions of the nanoparticles in paraffin were determined from the specific weight γ of the suspension using the following relations:

$$\eta_v = (\gamma - \rho_{par})/(\rho_{Gd} - \gamma), \quad (2)$$

$$\alpha_m = (\gamma - \rho_{par})\rho_{Gd}/(\rho_{Gd} - \rho_{par})\gamma, \quad (3)$$

where ρ_{Gd} and ρ_{par} are the densities of gadolinium and paraffin, respectively.

Suspension densities γ for all studied samples were close to the value that correspond to the same volume faction of Gd nanoparticles in paraffin (~1%). This was determined at an accuracy level of ±5%. The samples for studies of magnetism were prepared in the form of thin strips by squashing the solidifying suspension and poured into a thin-walled sealed container made of high-pressure polyethylene between two polished plates. The planar shape provided a significant decrease in the demagnetization factor when the sample was placed so that the directions of the constant magnetic field **H** and the alternating field **h** were parallel to the sample's main plane.

The same samples were used in measurements of the temperature dependence of the high-frequency permeability μ and the specific magnetization σ. The samples were placed in the nitrogen vapor heated to a given temperature and flowing through a double-walled glass tube with an evacuated layer. The magnetic state of the Gd nanoparticles near T_c was studied by analyzing the temperature dependence of the specific magnetization $\sigma(T)$ in the constant magnetic field H and of the high-frequency permeability $\mu(T)$ of the same samples at $H = 0$. The dependences $\sigma(T)$ were obtained using a vibration magnetometer; the polyethylene container with the sample was fastened to the vibrating quartz rod of the magnetometer.

Dependences of the permeability $\mu(T)$ were determined at the SHF ($\nu = 9.27$ GHz) using a volume resonator with the TE_{102} mode. The resonator was made from a silver-coated rectangular waveguide with the sizes 23×10 mm^2. The sample was inserted there along the axis of the temperature tube that crossed the resonator from one narrow side to the other narrow side at the central level. Holes with diameters of 9 mm were made on the narrow sides of the resonator for the tube to pass through. When the wide side of the resonator coincided with the direction of the magnetic component of the SHF field inside it, the Q factor achieved approximately 10^3. The Q factor decreased by ~0.3–0.5% when the sample was inserted into the resonator.

The task should be clarified, which was solved by measuring the permeability of Gd nanoparticles at high frequencies. It would be useful to mention earlier results obtained for these nanoparticles [18]. To start with, consider peculiarities of the structure of gadolinium nanoparticles and the effect of oxygen admixture on it.

A biphasic cubic structure is revealed by X-ray investigations (FCC1, FCC2) in nanoparticles with $d = 18$ nm, unlike the hexagonal structure typical of polycrystalline Gd samples. Large Gd nanoparticles of the sizes 89, 63, 47, and 28 nm possessed the HCP phase with an admixture of the FCC1 phase. The fraction of the cubic phase grew as the particle size decreased. The HCP structure in the nanoparticles corresponded perfectly to that of a macroscopic Gd sample. Surprisingly, the admixture of oxygen in the Gd nanoparticles at a level of up to 0.5 at % had no effect on their structure [18].

The studies of magnetic properties of Gd nanoparticles with the HCP structure conducted in [18–21] have revealed an important feature in the field dependences of the magnetization σ. It turned out that the curves $\sigma(H)$ show no hysteresis, i.e., $H_c \approx 0$. Therefore the basic, commonly accepted criterion for finding the critical size of the single-domain state from the maximum of the dependence of H_c on d does not work for nanoparticles. Moreover, no magnetic transition was observed in particles with sizes of 18 nm below T_c, and they remained in the paramagnetic state down to helium temperatures. In this situation, an idea was proposed to find the critical region of the single-domain state from the character of the dependence of the permeability μ on the nanoparticle size. It is known that, in ferromagnets, the process of moving domain walls makes the biggest contribution to their permeability μ and is responsible for the steepest segment of the magnetization curve. Rotation of magnetization in the domains provides the flatter segment of the magnetization curve; its contribution to the permeability of ferromagnetic compounds is weaker. The magnetization ultimately achieves saturation in a strong magnetic field, and any macroscopic sample becomes uniformly magnetized, i.e., it reaches a single-domain state; its magnetic permeability tends to zero.

As the size of nanoparticles decreases, the transition into the single-domain state in them can occur in the zero magnetic field. In a certain size range domain walls begin to disappear as the particles decrease in size and, hence, they become uniformly magnetized without the influence of the magnetic field; in other words, their magnetization in the zero field attains saturation. As a result, the permeability of these particles should decrease. That is why, in principle, the weakening of the dependence of μ in a certain size range of Gd nanoparticles can be used as a criterion for establishing the single-domain state.

The dependence $\mu(d)$ was obtained by observing the jump of the permeability of the particles with a certain size when they switched to the ferromagnetic state. In other words, it was constructed from the temperature dependence $\mu(T)$ when the sample tempera-

ture fell below T_c. To achieve the best agreement between the thermocouple readings and the sample temperature, one junction of the thermocouple was pressed directly into the sample volume. In addition, an automatic frequency adjustment system (AFAS) of the klystron to the resonance frequency of the resonator chamber was introduced between the resonator with the sample and the klystron generator. The $\mu(T)$ dependence was observed continuously, and the transition of the Gd nanoparticles into the ferromagnetic state was revealed as described below. A temperature change in the range $T < T_c$ led to a jump of the permeability value by $\Delta\mu_f(T)$, which resulted consequently in the shift of the resonator frequency (with the sample inside) by $\Delta\nu_f(T)$. Due to the feedback system, an unbalance signal $\Delta V_f(T)$ appeared on the klystron reflector, which corresponded to the resonator frequency shift. In the end, a linear correlation was established between the values of $\Delta V_f(T)$ and $\Delta\mu_f(T)$ for a small sample as follows:

$$\Delta V_f(T) = \alpha\Delta\mu_f(T). \quad (4)$$

In Eq. (4) α is a calibration constant. It may be estimated when the particles are in the paramagnetic phase ($T > T_c$). The point $T = 325$ K, which is 30 K higher than T_c, was chosen as a reference temperature for determining the paramagnetic state of the Gd particles and the values of ΔV_p and $\Delta\mu_p$. By applying the relation (4) to the paramagnetic state of the Gd nanoparticles, we can show that $\alpha = \Delta V_p/\Delta\mu_p$. Thus, it follows from Eq. (4) that

$$\Delta V_f(T)/\Delta V_p = \Delta\mu_f(T)/\Delta\mu_p. \quad (5)$$

Using the ratio of the electric signals at the klystron reflector that appear when the Gd nanoparticles transform from the para- to the ferromagnetic state, the relation between their permeabilities that correspond to this transition can be found. Note two main factors that led to the need to obtain the temperature dependences of the permeabilities for every particle size as the ratio $\Delta\mu_f(T)/\Delta\mu_p$. First, even a small inaccuracy in locating the sample in the SHF resonator significantly influences the frequency shift and hence the value of $\Delta\mu_f$. By normalizing $\Delta\mu_f$ by the permeability of the Gd particles $\Delta\mu_p$ in the paramagnetic state, we diminish the error caused by the inaccuracy of the sample location. Second, we did not aim to find the absolute values of the specific magnetization σ and the permeability $\Delta\mu_f$ of the Gd nanoparticles; we planned to study the influence of the temperature and the field H on the peculiarities of the magnetic transitions depending on the particle size and oxygen impurity. That is why the goal of the research was achieved despite a large error ($\pm 5\%$) of the volume fraction of the Gd particles in the samples.

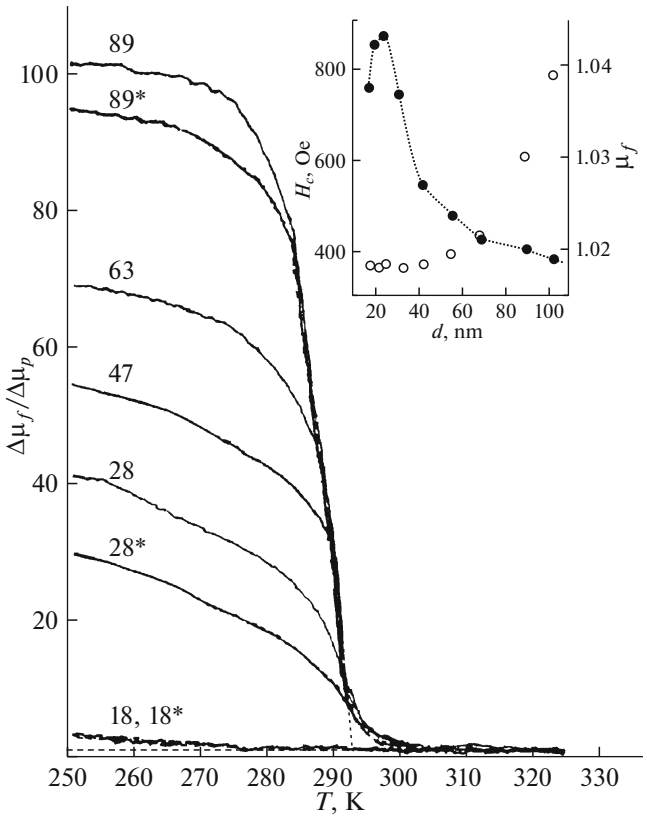

Fig. 1. Change in the relative magnetic permeability $\Delta\mu_f(T)/\Delta\mu_p$ of Gd nanoparticles as a function of T_c. Insert shows dependences of H_c (black circles) and μ_f (empty circles) for cobalt nanoparticles upon changing the size of the particles in the vicinity of transition into the single-domain state.

RESULTS AND DISCUSSION

Figure 1 shows the experimental dependences of the relative high-frequency permeability $\Delta\mu_f/\Delta\mu_p$ for the Gd nanoparticles of the sizes 89, 63, 47, 28, and 18 nm on the temperature in the vicinity of T_c. Analogous dependences for the sample with sizes of 89, 28, and 18 nm obtained with 0.5 mol % oxygen added in the helium flow, as described in [18], are marked with an asterisk. The dependences plotted in Fig. 1 were obtained by recording the voltage change ΔV_f at the klystron reflector when the sample temperature was changed from 325 to 250 K.

Before we analyze the dependences $\Delta\mu_f/\Delta\mu_p$ on T for the Gd nanoparticles shown in Fig. 1, let us consider the transition into the single-domain state of cobalt nanoparticles, which are a classical example of a uniaxial 3*d* ferromagnetic material. The purpose of this is to demonstrate and compare the transition into the single-domain state of Co nanoparticles by a change in their coercive force H_c and permeability μ_f. The insert in Fig. 1 shows the dependences of H_c (black circles) and of the high-frequency permeability

μ_f (empty circles) of the Co nanoparticles upon changing their size from 105 to 17 nm.

To simplify the comparison, the samples were also prepared as a suspension of Co nanoparticles in paraffin with the volume fraction of 1%. Producing the Co nanoparticles and their suspension in paraffin were conducted in strict agreement with the technology used for Gd nanoparticles [18]. However, the technology of sample preparation for measuring the permeability μ of the Co suspension at the SHF was modified according to the satisfactory resistance of cobalt to oxidation. Cylindrical samples had the diameter of 3 mm; their position in the center of the resonator was fixed very accurately using special inserts. As a standard for measuring absolute values of μ, samples made of polyethylene and pure paraffin of the same shape and size were used.

Evidently, H_c of Co particles grows continuously as the size d decreases and reaches the maximum near $d_0 \sim 25$ nm. In the range of $d < d_0$, the nanoparticles are in the single-domain state. This structure of the Co nanoparticles is consistent with the presence of a spontaneous magnetic moment, which is capable of coherent remagnetization under the influence of periodically changing magnetic field. There are a number of theoretical and experimental studies that prove the influence of the uniform magnetization of a $3d$ ferromagnetic nanoparticle on its hysteresis properties including the dependence of H_c on d [22].

The maximum on the dependence $H_c(d)$ and subsequent decrease as d grows further are due to a spontaneous remagnetization of the particles by either tunneling mechanism or caused by thermal oscillations (~kT) when the latter begin to dominate over the magnetic anisotropy energy of the particles.

The transition of the Co nanoparticles into the single-domain state is also proved by the weakening of the dependence of the permeability μ_f on the particle size when d is smaller than 60 nm. Apparently, domain walls disappear in particles of that size.

Consider the dependences $\Delta\mu_f/\Delta\mu_p$ presented in Fig. 1. The permeabilities of all Gd nanoparticles show a similar, almost identical smooth increase with T in a narrow temperature range (300–294 K), which can be attributed to the fluctuation ferromagnetism since, in this range, $T - T_c \ll T_c$ (see [16, chapter 47]). To study this and, in particular, to define the critical indices, special and more precise investigations are required.

Below T_c, the dependences $\Delta\mu_f(T)/\Delta\mu_p$ of the Gd nanoparticles with the size 28 nm and larger show a sharp increase in $\Delta\mu_f$ with T in a relatively narrow range ($\Delta T \sim 7$ K). A linear approximation of $\Delta\mu_f(T)$ until crossing the temperature axis allowed it to be estimated that $T_c = 293 \pm 1$ K. The value of T_c found in this manner coincides within the inaccuracy level with the paramagnetic Curie point $\theta = 292$ K, which was previously found in [18] from the dependence of χ^{-1} on T in the paramagnetic state of the nanoparticles.

It is evident from Fig. 1 that the value of the jump $\Delta\mu_1(T)$ depends on the particle size. For particles with sizes of 89 nm, the ratio $\Delta\mu_f(T)/\Delta\mu_p$ increases by almost 100 times in the considered temperature range and, for particles with $d = 28$ nm, the increase is only 20-fold. All studied nanoparticles have sizes which is almost two orders of magnitude smaller that the skin-layer thickness for gadolinium at the frequency $\nu \approx 10^{10}$ Hz, so the observed phenomenon cannot be explained by the inhomogeneity of the SHF field distribution inside the nanoparticle. This is also supported by the fact that the dependences $\Delta\mu(T)/\Delta\mu_p$ are almost identical in the paramagnetic state for the studied nanoparticles of all sizes.

An abrupt increase in $\Delta\mu_f(T)$ for the particles with $d = 89$ nm near T_c is undoubtedly attributed to the presence of domain walls in the particles.

At a temperature far away from the critical point T_c ($T < 280$ K), the dependences obtained for large particles ($d = 89$ and 63 nm) come to a plateau with a decrease in temperature and become independent of T below 270 K. The smaller particles ($d = 47$ and 28 nm) show dependences $\Delta\mu_f(T)/\Delta\mu_p$ close to linear as the temperature decreases (see Fig. 1).

Gadolinium nanoparticles of the same sizes obtained with addition of oxygen that have led to partial oxidation possess the same properties. The effect of the oxygen admixture on $\Delta\mu_f(T)/\Delta\mu_p$ for the particles with the size 89* and 28* nm manifests in a small decrease in the permeability of 89*-nm nanoparticles (and a more significant decrease for 28*-nm nanoparticles) far from T_c compared to the particles grown in pure helium. The addition of oxygen also decreased the magnetization of the particles but did not affect T_c and the paramagnetic Curie temperature [18].

It was shown above that the permeability of Co nanoparticles decreases as their size decreases in the region of the transition to the single-domain state, then it becomes size-independent (insert in Fig. 1). We might suggest that the behavior of the magnetization of Gd nanoparticles upon changing their sizes should change in a similar way if there is a transition into the single-domain state. However, the permeability of the Gd nanoparticles $\Delta\mu_f(d)$ in the same size range as for the Co particles behaves differently.

Finally, studies of the high-frequency permeability of the Gd nanoparticles with sizes of 89–18 nm can be assumed to not reveal any clear transition into the single-domain state. The absence of an unambiguous dependence of the permeability on the nanoparticle size for Gd may be related to the structural instability of the nanoparticles upon change in their size. At least the reasons for the structural transformation HCP–FCC1–FCC2 in the nanoparticles upon a decrease in

their size are still unclear [18]. The nature of magnetism in rare-earth metals is connected with the interactions of atomic *f* orbitals and conductivity electrons and, therefore, the large surface area of the nanoparticles can affect their structural stability.

The absence of a magnetic transition below T_c for nanoparticles with $d = 18$ nm can be qualitatively explained as follows. This phenomenon may be related to a violation of the RKKY (Ruderman–Kittel–Kasuya–Yosida) interactions, which is usually assumed to cause magnetic ordering in rare-earth metals. According to the RKKY theory, magnetic interaction between remote 4*f* ion shells can only occur indirectly due to the polarization of conductivity electrons. In nanoparticles with diameters of ~10 nm, conductivity electrons can lose their polarization in short times ($\tau \sim 10^{-11}$ s) due to collisions with the particle surface. This fact, as well as an increase in the distance between the 4*f* ions in nanoparticles upon the transition from the HCP to the FCC structure, should also weaken the RKKY interaction and, hence, influence the magnetic state of the particles.

Consider further the influence of the temperature on the magnetization of Gd particles in the constant magnetic field. It is known that gadolinium should possess a uniaxial magnetic anisotropy due to the hexagonal lattice structure; the anisotropy energy can be written as follows allowing for the first two series terms:

$$U_{an} = K_1 \sin^2 \Theta + K_2 \sin^4 \Theta. \quad (6)$$

Here, K_1 and K_2 are the first and second constants of the magnetic anisotropy and Θ is the angle between the easy magnetization axis (z axis) and the direction of the magnetic field H. A peculiarity of gadolinium is its specific temperature behavior of the first constant K_1. The dependences $K_1(T)$ and $K_2(T)$ for Gd in the temperature range 300–180 K taken from [15] are presented in Fig. 2. The character of the dependences leads to a conclusion that at $T > 240$ K gadolinium is a classical uniaxial ferromagnet ($K_1 > 0$, $K_2 \sim 0$), and below 240 K an orientation transition takes place. The dependence $K_1(T)$ passes through zero and continues to decrease in the negative region. As a result, both the direction of the spontaneous magnetization of gadolinium and the symmetry of its magnetic structure change [16]. Instead of the uniaxial magnetic anisotropy with an easy axis which defines the coercivity of gadolinium at $T > 240$ K, another anisotropy type is established (easy plane). In this plane (which is the x–y basis plane of the crystal) the magnetization can freely change its direction without leaving the basis plane under the influence of a small field H. However, correlation (6) shows that there is a second term in the expansion of the anisotropy energy K_2 that can also influence the direction of the magnetization vector in gadolinium. It was theoretically supposed that the orientation transition in gadolinium can be induced by the field H [16].

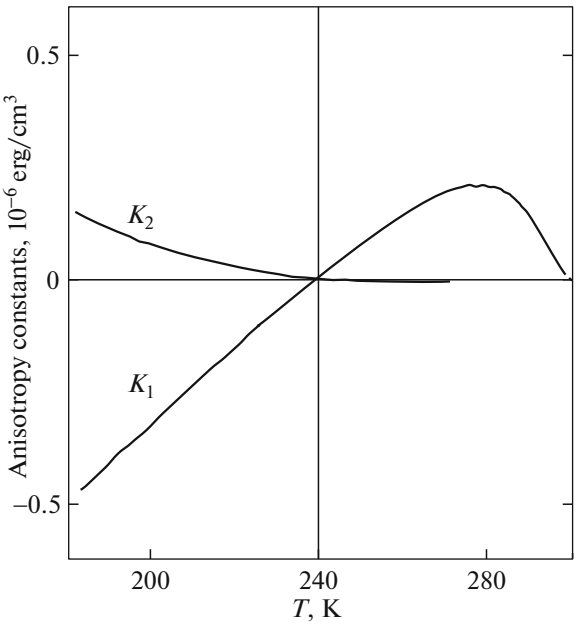

Fig. 2. Dependences of the anisotropy constants K_1 and K_2 of gadolinium on the temperature near T_c [15].

The above discussion is applied to the magnetic anisotropy and magnetism of a macroscopic gadolinium crystal. A completely different scenario can take place in Gd nanoparticles. Figure 3 shows the dependences of the specific magnetization $\sigma(T)$ of ensembles of Gd nanoparticles that have different sizes and, for comparison, of a polycrystalline sample magnetized in the field with an intensity of (a) 4×10^2, (b) 4×10^3, (c) 4×10^4, and (d) 4×10^5 A m^{-1}. The dependences $\sigma_b(T)$ for the polycrystalline gadolinium sample are drawn with dashed lines for comparison. To simplify the comparison of the dependences $\sigma(T)$ and $\sigma_b(T)$, the vertical scale of $\sigma_b(T)$ is decreased, and the scaling factor is written as a fraction above every curve $\sigma_b(T)$.

When the samples are magnetized in a weak magnetic field (Fig. 3a) only ten times higher than the Earth's field ($H_E \approx 40$ A m^{-1}), the dependences $\sigma_b(T)$ and $\sigma(T)$ of the nanoparticles with $d = 89$ nm have one maximum each, which resemble each other and appear at different temperatures. The plots of $\sigma(T)$ in the same weak field for particles 63, 47, and 28 nm in diameter are completely different (Fig. 3a). They are similar and, after a sharp increase near T_c, continue to grow smoothly without any jumps as the temperature decreases.

When the field is increased ten times or more, ensembles of nanoparticles that differ in size show a smooth enhancement of the $\sigma(T)$ dependences (Figs. 3b–3d), which is very similar to the behavior of

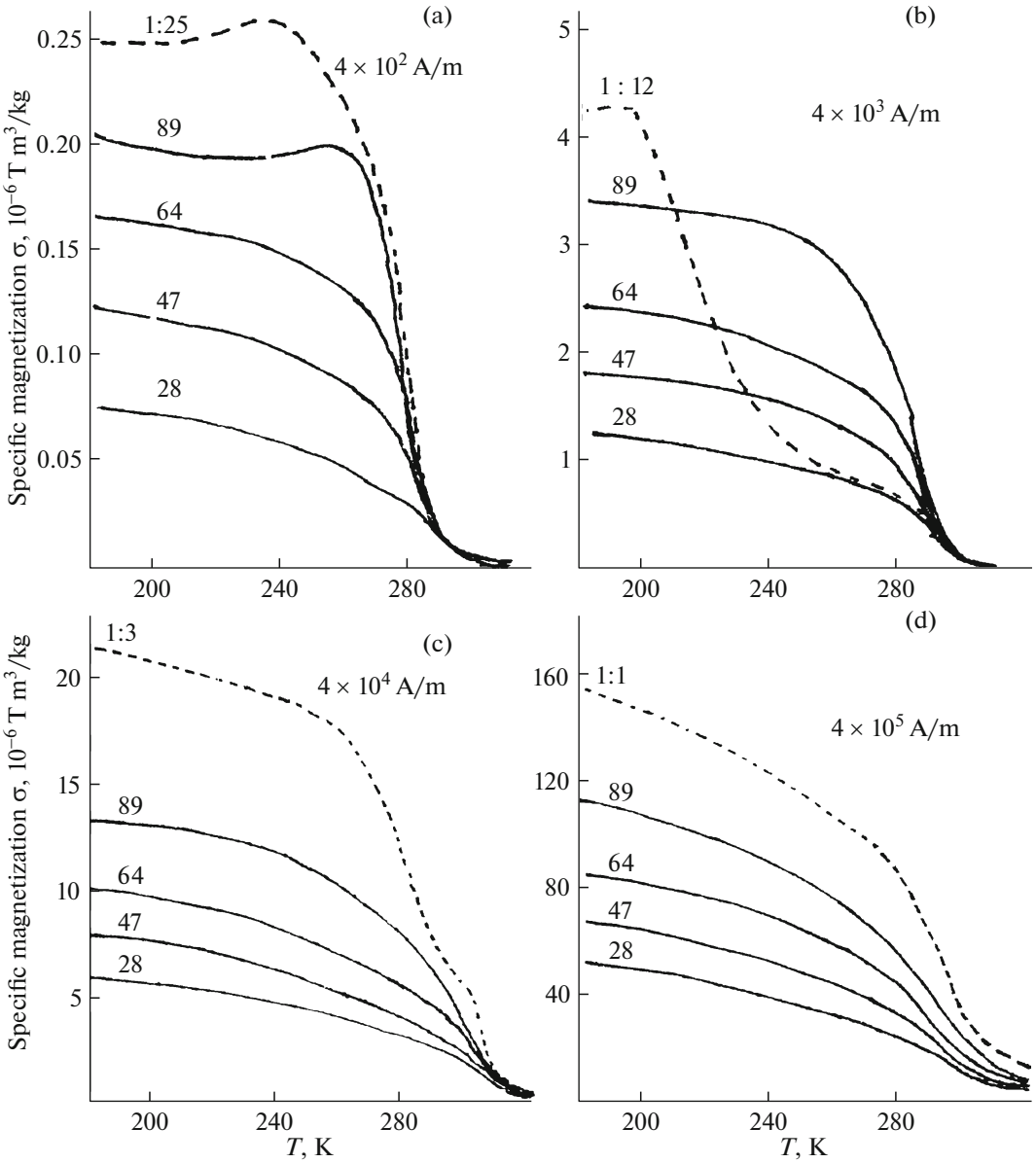

Fig. 3. Dependences of specific magnetization $\sigma(T)$ for nanoparticles with sizes of 89, 64, 47, and 28 nm in magnetic field with intensity H of (a) 4×10^2, (b) 4×10^3, (c) 4×10^4, and (d) 4×10^5 A m^{-1}. Dashed lines represent $\sigma(T)$ for macroscopic Gd sample with scaling factor indicated (for convenience of comparison with $\sigma(T)$ dependences for Gd nanoparticles of different sizes).

nanoparticles smaller than 63 nm in the weak field ($H = 4 \times 10^2$ A m^{-1}) presented in Fig. 3a. Note that the maximum in $\sigma(T)$ for 89-nm particles disappears, and this dependence becomes analogous to $\sigma(T)$ of smaller nanoparticles.

The field $H = 4 \times 10^3$ A m^{-1} has the maximal effect on $\sigma_b(T)$. Figure 3b demonstrates a sharp increase in $\sigma_b(T)$ below 240 K, which is actually the temperature range where the constant K_1 passes through zero and Gd is transformed from a uniaxial magnetic ($K_1 > 0$) to an easy-plane type magnetic ($K_1 < 0$). Note that the function $\sigma_b(T)$ of a macroscopic sample near 240 K differs noticeably from the $\sigma(T)$ dependences of Gd nanoparticles, which show a smooth and similar character of the magnetization increase at decreasing T.

It is evident from Fig. 3d that, in the strongest field ($H = 4 \times 10^5$ A m^{-1}), all dependences $\sigma(T)$ of the nanoparticles and $\sigma_b(T)$ of the polycrystalline Gd sample have the same shape. They are similar to the dependences $\sigma(T)$ for the nanoparticles with $d = 63$, 47, and 28 nm magnetized in the lowest field 4×10^2 A m^{-1} (Fig. 3a) and to $\sigma(T)$ for all studied Gd nanoparticles in the intermediate fields H (Figs. 3b, 3c).

A comparison of the curves $\sigma(T)$ and $\sigma_b(T)$ presented in Fig. 3 allows us to draw certain conclusions. Consider first the influence of the field on the magne-

tism of the polycrystalline Gd sample, the dependence of which $\sigma_b(T)$ is shown in Fig. 3 by dashed lines. Figures 3a–3c show that these dependences have different bends, the positions of which are unambiguously related only to the effect of T and H on the constant K_1. Their influence on K_2 can be neglected, since, in the temperature range of T_c up to 180 K, the value of K_1 is much higher than K_2 (functions $K_1(T)$ and $K_2(T)$ are plotted in Fig. 2). At $H = 4 \times 10^5$ A m^{-1} (Fig. 3d), all bends in $\sigma_b(T)$ disappear, and the curve shows simple smooth growth as the temperature decreases. A further increase in the field H to 8×10^5 A m^{-1} has no effect on the character of the dependence $\sigma_b(T)$.

An increase in the magnetizing field to $H = 4 \times 10^5$ A m^{-1} leads to the disappearance of domain walls in the sample of polycrystalline gadolinium placed in that field; the sample acquires uniform magnetization or, in other words, comes to the single-domain state. That is why it can be assumed that the magnetic structure of the Gd polycrystal, rather than the magnetic field itself, stimulates the orientation transition. This may be the first experimental proof of an orientation transition stimulated by the magnetic field.

To reveal the magnetic structure of Gd nanoparticles, compare the dependences $\sigma(T)$ of nanoparticles with sizes of 63 nm and lower magnetizations in a weak magnetic field $H \approx 0$ (Fig. 3a) with the dependence $\sigma_b(T)$ of the polycrystalline Gd sample magnetized in a high field $H = 4 \times 10^5$ A m^{-1} (Fig. 3d). These dependences are similar, though polycrystalline Gd is magnetized in a strong field almost to saturation, and nanoparticle ensembles show an adequate magnetization level but in almost zero field. This indicates that the ensembles contain spontaneously magnetized particles that can be assumed to be in the single-domain state. Only a small fraction of these particles in the ensemble have the basis place that coincides with the direction of the external magnetic field. Therefore, the total magnetization of the nanoparticle ensemble along the H direction remains small.

It is possible to assume that a polycrystalline Gd sample in an intense field is an ensemble of single-domain crystallites, the easy magnetization directions of which lie in their basis planes ($K < 0$), which are chaotically distributed in space. The sum of projections of their magnetizations on the direction of the magnetic field is then the total magnetization of the sample. On the other hand, if magnetic interactions between the crystallites are neglected, which is quite possible near T_c, then the magnetic structure of this sample is nearly equivalent to an ensemble of nanoparticles that has easy-plane type anisotropy ($K_1 < 0$) with chaotically distributed orientations of their basis planes in space.

The dependence of magnetization on the field H for ensembles of nanoparticles with easy-plane type anisotropy ($K_1 < 0$) was recently calculated theoretically [22]; in the case of these nanoparticles, cyclic remagnetization curves were shown not to have hysteresis. This agrees well with the experimental studies of magnetism of both the polycrystalline sample and Gd nanoparticles.

CONCLUSIONS

As a result of a comparative study of the magnetic properties of the polycrystalline sample and spherical nanoparticles of gadolinium with the sizes of 89, 63, 47, 28, and 18 nm in the vicinity of T_c, the influence of magnetic field H on the temperature dependence of the magnetization was experimentally found in the macroscopic sample and 89-nm nanoparticles. No influence of H on the character of the dependences $\sigma(T)$ was found for nanoparticles 63, 47, and 28 nm in diameter. The dependences $\sigma(T)$ of the nanoparticles in the zero field and $\sigma_b(T)$ of the polycrystalline sample in the intense field are found to be similar near T_c. It is suggested that nanoparticles with HCP structure and sizes of 63 nm and smaller have spontaneous magnetization, i.e., are in the single-domain state. In the vicinity of T_c, these nanoparticles immediately achieve easy-plane-type anisotropy and, in the polycrystalline sample, a transformation of this kind only occurs when it is magnetized in a high magnetic field.

ACKNOWLEDGMENTS

Author thanks A.P. Aleksandrov, I.P. Lavrent'ev, D.A. Kulakov, P.A. Kulakov, A.V. Petinova, and V.V. Shevchenko for their assistance in the work and useful discussions.

REFERENCES

1. A. M. Tichin and Y. I. Spichkin, *Magnetocaloric Effect and Its Applications* (IOP Publishing, London, 2003).
2. C.-J. Hsu, S. M. Sandoval, K. P. Wetzlar, and G. P. Carman, J. Appl. Phys. **110**, 123923 (2011).
3. Y. Fukumori and Y. H. Ichikawa, Adv. Powder Technol. **17**, 1 (2006).
4. J. A. Nelson, L. H. Bennett, and M. J. Wagner, J. Am. Chem. Soc. **124**, 2979 (2002).
5. P. Z. Si, I. Skorvanec, J. Kovac, D. Y. Geng, X. G. Zhao, and Z. D. Zhang, J. Appl. Phys. **94**, 6779 (2003).
6. Z. C. Yan, Y. H. Huang, Y. Zhang, H. Y. Okumura, J. Q. Xiao, S. Stoyanov, V. Skumraev, G. C. Hadjipanayis, and C. Nelson, Phys. Rev. B **67**, 054403 (2003).
7. O. Starikov and K. Sakurai, Vacuum **80**, 117 (2005).
8. Y. Fukumori and H. Ichikawa, Adv. Powder Technol. **17**, 1 (2006).
9. X. G. Liu, D. Y. Geng, Q. Zhang, J. J. Jiang, W. Liu, and Z. D. Zhang, Appl. Phys. Lett. **94**, 103104 (2009).
10. C.-J. Hsu, S. V. Prikhodko, C.-Y. Wang, L. J. Chen, and G. P. Carman, J. Appl. Phys. **111**, 053916 (2012).

11. I. A. Aleksandrov, I. Yu. Metlenkova, S. S. Abramchuk, S. P. Solodovnikov, A. A. Khodak, S. B. Zezin, and A. I. Aleksandrov, Tech. Phys. **58**, 375 (2013).
12. B. Issa, I. M. Obaidat, B. A. Albiss, and Y. Haik, Int. J. Mol. Sci. **14**, 21266 (2013).
13. S. Hou, S. Tong Hou, J. Zhou, and G. Bao, Nanomedicine **7**, 211 (2012).
14. M. O. Oyewumi, R. A. Yokel, M. Jay, T. Coakley, and R. J. Mumper, J. Controlled Release **95**, 613 (2004).
15. K. N. R. Taylor and M. I. Darby, *Physics of Rare Earth Solids* (Springer, 1972).
16. L. D. Landau and E. M. Lifshitz, *Electrodynamics of Continuous Media* (Nauka, Moscow, 1982, Butterworth-Heinemann, 1984), p. 228.
17. M. Ya. Gen and A. V. Miller, Poverkhnost **2**, 150 (1983).
18. V. I. Petinov, Russ. J. Phys. Chem. A **90**, 1413 (2016).
19. M. Ya. Gen, A. N. Kostygov, V. I. Petinov, A. E. Petrov, and N. I. Stoenko, Fiz. Tverd. Tela **17**, 2760 (1975).
20. Yu. G. Morozov, A. N. Kostygov, V. I. Petinov, and P. E. Chizhov, Phys. Status Solidi A **32**, K119 (1975).
21. P. E. Chizhov, A. N. Kostygov, and V. I. Petinov, Solid State Commun. **42**, 323 (1982).
22. V. I. Petinov, Tech. Phys. **59**, 6 (2014).

Translated by S. Efimov